EurJIC
European Journal of Inorganic Chemistry

Research Article
doi.org/10.1002/ejic.202200027

Chemistry Europe
European Chemical Societies Publishing

www.eurjic.org

Bis-Anagostic Structures in N,N'-Chelate Ligand Complexes of Palladium(II)

M. Arif Sajjad,[a] Peter Schwerdtfeger,[b] Yichao Cai,[c] Joyce M. Waters,[c] John A. Harrison,*[c] and Alastair J. Nielson*[c]

Reaction of N,N'-dibenzylidene-2,2-dimethylpropylenediamine with $Pd(OAc)_2$ produces essentially one product which NMR spectroscopy indicates has a *bis*-anagostic structure. A density functional theory (DFT) calculation shows that in the square planar structure, both aromatic rings lie above the coordination plane with close approaches of two *ortho*-C–H bond hydrogens to both the Pd centre and the two acetato ligand coordinating oxygen atoms. N,N'-dibenzylideneethylenediamine reacts with $Pd(OAc)_2$ similarly where a *bis*-anagostic structure is indicated by NMR spectroscopy and a DFT calculation shows an energy preference for an above plane positioning of the two aromatic rings. N,N,N',N'-tetrabenzylethylenediamine reacts with $Pd(OAc)_2$ to give a structure which X-ray crystallography shows two benzyl phenyl groups lie above and below the coordination plane respectively.

Introduction

Cyclometallation reactions[1] are now an important part of organic synthesis in that ligand directed reactions can be carried out for a variety of functional groups that achieve new functional group imposition on post functionalisation of the metal–carbon bond. Cyclopalladated complexes are particularly important in this field as C–H bond activation can be readily achieved[2] but due to the cost of palladium, alternative systems are continually being developed to overcome this problem.[3]

In general, reactions which result in functionalised aromatic rings that employ cyclopalladations involve the implementation of one palladium centre per organic substrate. However, a further way of reducing the amount of an expensive transition metal and achieving efficiency would be to generate two Pd–C bonds on the same metal centre using a bidentate ligand (Scheme 1) and then carry out the functionalisation of both.

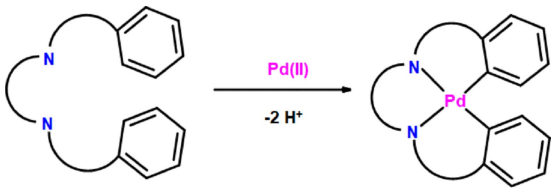

Scheme 1. Bidentate ligand *bis*-cyclopalladation.

Stable *bis*-cyclopalladated complexes can be generated from *ortho*-lithiated organic compounds using two equivalents of the reagent with $PdCl_2$,[4] from *ortho*-mercurated organic compounds,[5] from *trans*-amine $PdCl_2$ complexes,[6] or by conversion from other complexes.[7] However, achieving bifunctional cyclopalladates through processes similar to mono-cyclopalladation has only been achieved for *ortho*-benzylic CH_3 groups and mono-cyclopalladation of *ortho*-aromatic C–H groups appears to halt at this stage.[8] Given that *bis*-cyclopalladated complexes are known to undergo insertion reactions into the Pd–C bonds,[4d,h] and that there is easy access to a variety of bifunctional chelating ligands and also given the importance of ligand-directed C–H bond activation using bidentate ligands[9] as well as the desirability for cost reduction, it appeared to us that the single report on the reluctance of this type of reaction to produce *bis*-cyclopalladated complexes using bidentate amine ligands,[8] deserved further scrutiny. In the work presented here, we look at some of the underlying aspects involved in the attempted preparation of *bis*-cyclopalladated complexes using N,N'-diimine chelates.

Results and Discussion

For the purposes of the present study, we have used propylene and ethylene diimine N,N'-chelates (Figure 1) to vary the backbone structure of potential ligands that might undergo *bis*-

[a] Dr. M. A. Sajjad
Department of Chemistry, Division of Science and Technology,
University of Education, Lahore, 54000, Pakistan
E-mail: arif.sajjad@ue.edu.pk
[b] Prof. Dr. P. Schwerdtfeger
Centre for Theoretical Chemistry and Physics,
Institute of Advanced Studies,
Massey University Auckland,
Private bag 102904, North Shore Mail centre, Auckland, New Zealand
E-mail: peter.schwerdtfeger@gmail.com
[c] Y. Cai, J. M. Waters, Dr. J. A. Harrison, Prof. Dr. A. J. Nielson
School of Natural Sciences,
Massey University Auckland,
Private bag 102904, North Shore Mail centre, Auckland, New Zealand
E-mail: j.waters@massey.ac.nz
j.a.harrison@massey.ac.nz
a.j.nielson@massey.ac.nz

Supporting information for this article is available on the WWW under https://doi.org/10.1002/ejic.202200027

Research Article
doi.org/10.1002/ejic.202200027

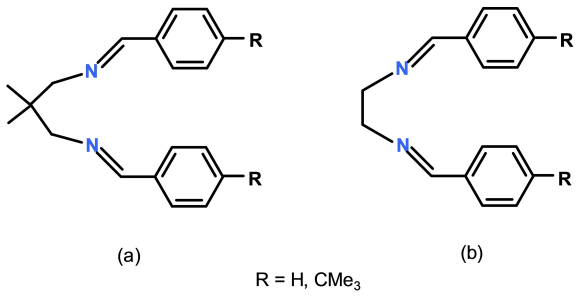

Figure 1. Diimine N,N′-chelate ligands used in the reactions with $Pd(OAc)_2$. (a) propylene diimine bridge, (b) ethylene diimine bridge.

cyclopalladation. We have then used palladium acetate for the reactions rather than palladium chloride used in the previous bidentate amine study[8] due to the well-known ability for the acetato ligand to act as a proton acceptor for the C–H bond activation in the Concerted Metallation Deprotonation/Ambiphilic Metal Ligand Activation (CMD/AMLA) mechanism of cyclopalladation[10] which might then facilitate the formation of two Pd–C bonds.

To conserve the palladium, reactions were carried out on a scale that was just sufficient to use NMR spectroscopy to look at the products and thus determine the nature of any coordination compounds that might be present. The NMR tube solution was then layered with an appropriate solvent in an attempt to obtain crystalline reaction products that could then be subject to X-ray analysis. Whether this was achieved or not, we have also used DFT calculations to yield structures and thus reveal any inherent features that might be used to progress the reaction.

Synthesis, NMR Spectra and Structures

Addition of 2,2-dibenzylidene-2,2-dimethylpropylenediamine [Figure 1a, R = H] to $Pd(OAc)_2$ in a 1:1 ratio in methanol and stirring the reaction overnight led to a lightening of the solution colour but no precipitate was formed. Trace quantities of palladium metal were also produced during the reaction. Removal of the solvent led to a yellow solid for which the NMR spectra showed that one major complex was produced in amongst a variety some minor products that were also present. A reaction whereby the reactants were stirred in $CHCl_3$ overnight or refluxed in CH_2Cl_2 overnight, produced a similar yellow solid on work-up where the NMR spectra indicated there was essentially only the more abundant product that was found for the methanol reaction (see Figure S2a in the ESI for these spectra).

In the ^{1}H NMR spectra, there were methyl group singlets for the propylene chelate back-bone and acetato ligands in a 1:1 ratio indicating that there were two of the latter ligands and a symmetrical structure was present. However, the single resonance for the chelate back-bone CH_2 groups for the free ligand was now split into a well separated but poorly resolved AB quartet system indicating again symmetry for two sides of the ligand but that the two H atoms on each side are diastereotopic as they experience different chemical environments. In the aromatic region, there was a single set of resonances for each of the *ortho*, *para* and *meta* hydrogens of both aromatic rings and one resonance for the two imine CH protons all of which reflects symmetry in the molecule. A particular feature of this region of the spectrum however is that the *ortho*-protons show a downfield shift of approximately 1.1 ppm in comparison to the free ligand which is characteristic of anagostic interactions that are found in the initial coordination stage of cyclopalladation reactions involving monodentate ligands.[11a,b] With only one resonance for the 2 *ortho*-protons on each side of the chelate, the aromatic rings must be rapidly rotating on the NMR time scale.

As the ^{1}H NMR spectrum indicates a symmetrical molecule, it then suggests that the symmetry may arise from two possible anagostic structures whereby both aromatic rings are positioned above the coordination plane or one above and one below. In an attempt to rationalise this situation, we layered the NMR tube $CDCl_3$ solution with $CHCl_3$ and then diethyl ether or a variety of non-polar solvents, but no crystalline material was forthcoming. This process often produced further palladium metal and darkening of the solution along with the production of gummy droplets. Thus, to obtain anagostic structural information, a DFT structure was calculated whereby the C–H bond lengths could then be used to produce realistic separation distances for any close approaches that might be present compared to what can be achieved from X-ray structures.

The energy minimised structure **1**, is shown in Figure 2 where it is seen that both aromatic rings lie above the coordination plane. No energy minimisation of a structure involving above and below plane aromatic rings was attempted as molecular models indicate that the propylene linker would form an improbable boat structure which would not reflect the symmetry indicated by the ^{1}H NMR spectrum. The structure of **1** consists of a square planar coordination geometry with two sets of *trans*-related N atoms of the chelating diimine ligand and O atoms of two terminal acetato ligands. With the nitrogen atoms of the chelate coordinated to Pd, a six-membered ring is formed

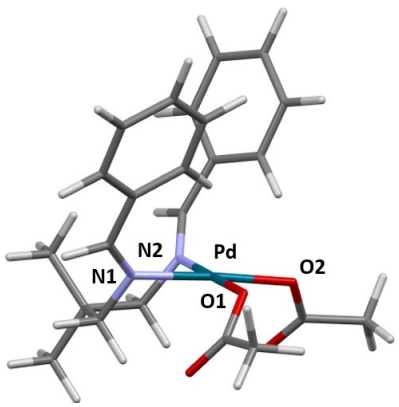

Figure 2. DFT calculated structure of complex **1**. Selected bond lengths (Å) and angles (°): Pd–N1 2.009, Pd–N2 2.014, Pd–O1 2.011, Pd–O2 2.019; Pd–N1=CH 130.8, Pd–N2=CH 131.0, N1=CH–C 128.1, N2=CH–C 128.2.

Research Article
doi.org/10.1002/ejic.202200027

which adopts a chair conformation where the 3-carbon section of the propyl bridge lies behind and below the coordination plane. This conformation then dictates that the two imine carbon atoms point upwards above the coordination plane which results in both aromatic rings also lying above the coordination plane. The remainder of the molecule consists of the two acetato ligands where the Pd–O bond rotations are such that each C=O group oxygen lies below the coordination plane. The overall symmetry shown by this calculated structure is then consistent with the ^{1}H NMR spectrum that was observed for the major reaction product.

With both aromatic rings lying above the coordination plane in **1**, the Pd–N=CH angles (130.8 and 131.0°) are significantly larger than the sp^2 angle of 120°, as are the N=CH–C_{ipso} angles (128.1 and 128.2°). In this situation where the calculation produces a frozen structure, one of the aromatic rings is rotated more than the other with respect to the position above the coordination plane so that the N1=CH–C_{ipso}–C_{ortho} torsion angle (i.e. the C_{ipso}–C=N 'twist' angle) is 10.0° so that the ring is rotated upwards out of the Pd–N1=CH plane. For the other aromatic ring, this torsion angle is 23.4° with the rotation downwards of the Pd–N1=C plane (see the torsion angle depictions in Figure S3 of the ESI. Bond lengths and angles are in Table S1 of the ESI).

The locked-in rotations of the aromatic rings in the structure then place one *ortho*-hydrogen of each ring in slightly different positions above the coordination plane where they make close approaches to the metal centre of 2.418 and 2.644 Å (Figure 3). These short Pd···H–C separations are consistent with anagostic interactions for Pd[11] but are unique in that they involve two aromatic rings in an above-plane orientation. This structural feature contrasts with above and below orientations of aromatic rings that have been observed by X-ray crystallography for palladium.[11f–h] In solution however, the observation of the downfield shift for all 4 *ortho*-hydrogens shows that there is room for the aromatic rings to fully rotate. The structure also shows there are relatively close approaches of the two *ortho*-hydrogens and the acetato ligand coordinated oxygen atoms where the O···H–C separations are 2.775 and 2.115 Å. With both Pd···H–C and O···H–C close separations being present, the C–H bond distances involving the two interactions at 1.093 and 1.091 Å are marginally shorter than the other aromatic ring C–H bond distances (range 1.099 to 1.102 Å) but the H–C–C–H torsion angles (how the C–H bond deviates from the plane of the aromatic ring) are little different to the others.

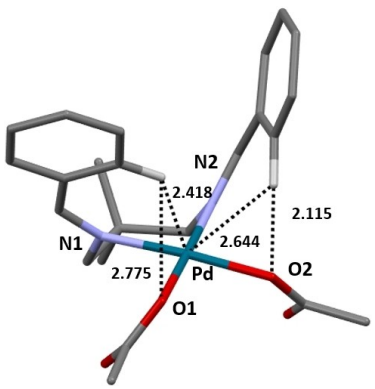

Figure 3. Close approaches of the *ortho*-hydrogen atoms to the Pd centre and the coordinated O atoms in complex **1**.

We have then used QTAIM analysis which gives a topological description of the electron density[12] and NBO analysis which gives a localised bonding description in terms of Natural Bond Orbitals (NBO's),[13] to unravel the bonding characteristics involved with the close separations. Although the NMR spectra show that there is a time-averaged downfield anagostic shift for the 4 *ortho*-protons of the two aromatic rings, the DFT structure produces the lowest energy 'frozen' structure which for complex **1** has one short Pd···H–C contact (2.418 Å) and this interaction shows a bond critical point (bcp) in the QTAIM analysis (see the molecular graph in fig S4 of the ESI) and other QTAIM features (Table S2 in the ESI) that are in accord with other anagostic interactions we have studied[11]. However, the longer Pd···H–C separation for the other aromatic ring (2.644 Å) does not show a bcp but this is not unusual as the QTAIM analysis can avoid areas of lower electron density[12d]. There is also a bcp for the short O2···H–C contact (2.115 Å) involving the other aromatic ring and the *ortho*-hydrogen. In addition, the QTAIM H-atomic charges (full values in Table S3 of the ESI) for the 2 interacting *ortho*-hydrogens with *q*(H) values of 0.057 and 0.102 a.u., are significantly more positive than the two other non-interacting *ortho*-hydrogens [*q*(H) values 0.018 and 0.016 a.u.] as well as the other remaining ring hydrogens [range of *q*(H) values, 0.023 to 0.027 a.u.]. In these cases, the two more positively charged hydrogens form weak repulsive Coulombic interactions with palladium [*q*(Pd), 0.853 a.u.] and weakly attractive Coulombic interactions with the adjacent oxygen atoms [*q*(O) values, −1.037 and −1.049 a.u.]. Interestingly, the larger *ortho*-hydrogen interaction *q*(H) value of 0.102 a.u., corresponds to the shorter O2···H–C separation (2.115 Å), and the smaller *q*(H) value (0.057 a.u.) with the longer Pd···H–C contact (2.644 Å).

For the NBO analysis, there are C–Hσ to Pd d hybrid orbital donations for each Pd···H–C separation but the values for the second order perturbation energy [*E*(2) of only 3.1 and 1.8 kcal mol^{-1}] are typical of other anagostic interactions we have studied.[11] In terms of NBO analysis, the values are somewhat below the realistic working level for the method, but they are included here for completeness. For example, in comparison, the *E*(2) values for the much stronger nitrogen lone-pair to palladium donations are 243.1 and 246.0 kcal mol^{-1}. However, there is considerable Pd to C–Hσ* orbital back donation for the closer Pd···H–C separation of 2.418 Å where the *E*(2) value is 10.1 kcal mol^{-1} but for the other Pd···H–C separation of 2.644 Å the *E*(2) value is only 3.0 kcal mol^{-1}. Interestingly, although the O2···H–C separation is short at 2.115 Å, there is no O2p to C–Hσ* orbital donation observed so that this weak hydrogen bond interaction would appear to be Coulombic in nature but again very weak [*q*(H) and *q*(O) values of 0.102 and −1.049 a.u. respectively].

In passing, we also note that the QTAIM molecular graph for complex **1** shows a bcp between both of the acetato ligand

Research Article
doi.org/10.1002/ejic.202200027

C=O oxygens with the C–H bond hydrogens of the propylene bridge structure that lies adjacent to them in the frozen structure that is developed. In these cases, the O···H–C separations are quite short at 2.408 and 2.370 Å and the particular C–H bond lengths for these axial hydrogens of the chair structure at 1.108 and 1.107 Å are somewhat shorter than the C–H bond lengths for the equatorial hydrogens (1.113 and 1.112 Å respectively). For the axial hydrogens the *q*(H) values are 0.089 and 0.092 a.u. which with the *q*(O) values of −1.162 and −1.159 a.u. again represent weak hydrogen bonds. However, the NBO analysis shows that there are no relevant orbital donations associated with the interactions so that they would appear to be electrostatic in nature only.

We have also looked at *para*-substituted diimine ligands and found that this type of ligand produced downfield shifted *ortho*-hydrogen spectral features similar to the unsubstituted molecule when reacted with $Pd(OAc)_2$ in methanol or $CHCl_3$. In particular, the *para-tert*-butyl substituted chelate [Figure 1a, R = CMe_3] produced a spectrum whereby the 4 *ortho*-hydrogens appeared as a single down-shifted doublet in the ^{1}H NMR spectrum in comparison to the free ligand (see Figure S1 in the ESI). When the NMR solution was layered with $CHCl_3$ and diethyl ether, some yellow crystalline material was obtained but final refinement of the X-ray structure was precluded by an apparently unsolvable disorder problem of one of the propane N,N′-diimine methyl groups. However, at the stage of refinement achieved, the structure did show that both aromatic rings lie above the coordination plane as the calculated structure for complex **1** had indicated (see the structure in Figure S5 of the ESI).

We have also made reaction studies of bidentate imine ligands with $Pd(OAc)_2$ where the N,N′ bridge is CH_2–CH_2 (ethylene bridge) in order to ascertain if the shortening has any structural effect. When either the dibenzaldimine or di-*para-tert*-butylbenzaldimine ligands (Figure 1b) were stirred in methanol with one equivalent of $Pd(OAc)_2$ overnight, the NMR spectra indicated that a variety of products are formed but there are fewer of these when the reactants are stirred in CH_2Cl_2 overnight (see Figures 2Sc and 2Sd in the ESI). This contrasts with the propylene diimine reactions where the main products were the *bis*-anagostic complexes. As the reactions also produced significant palladium black especially on attempted recrystallisation, indicating oxidation was occurring, no attempt was made to characterise all the products by NMR spectroscopy. The spectra do however show downfield shifted *ortho*-hydrogen doublets for one of the more significant products in each reaction which are consistent with anagostic interactions being present. Unfortunately, layering of the NMR tube solutions with low polarity solvents has not produced any crystalline material for any of the products and an additional complication is that this process produces further palladium metal.

To uncover the likely anagostic structure that is found among the various products in the synthetic reactions, we have carried out a calculation of the NCH_2CH_2N dibenzaldimine coordinated to $Pd(OAc)_2$. The energy minimised structure that was obtained for this complex **2**, is shown in Figure 4, where it

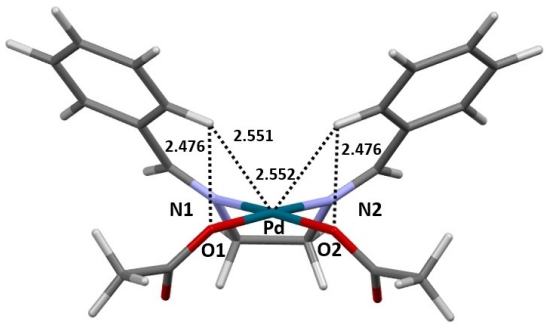

Figure 4. Calculated structure of dibenzaldimine complex **2** showing the Pd···H–C and Pd···O separations (Å). Selected bond lengths (Å) and angles (°): Pd–N1 2.010, Pd–N2 2.009, Pd–O1 2.009, Pd–O2 2.009; Pd–N1=CH 136.3, Pd–N2=CH 136.3, N1=CH–C 127.8, N2=CH–C 128.8; torsion angles (°): Pd–N=CH–C 0.3, N=CH–C–CH 11.0.

is seen that again, both aromatic rings lie above the coordination plane. The complex is symmetric on both sides of the central Pd atom, and this arises when the ethylene bridge carbons of the N,N′ chelate five membered ring both lie below the coordination plane where the N–C–C–N section is planar and the N–Pd–N section is puckered.

With the Pd–N=CH–C_{ipso} and N=CH–C_{ipso}–C_{ortho} torsion angles being 0.3 and 11.0° respectively, the aromatic rings are rotated so that the C–H hydrogens of the two rotation-frozen rings lie above the coordination plane and are positioned more over the top of palladium than the oxygen atoms. In this situation, the Pd···H–C separations are 2.551 Å but because the aromatic rings are inclined towards the coordination plane (aromatic ring/coordination plane angle 50.1°) the H···O distances are a little shorter at 2.476 Å.

QTAIM analysis for above-plane aromatic ring complex **2** shows that with the two *ortho*-hydrogens lying essentially above the palladium centre, there are two bcp's associated with the short Pd···H–C separations (2.552 Å) but no bcp's for the O···H–C separations of 2.476 Å with the QTAIM *q*(H) and *q*(Pd) values of 0.063 and 0.858 a.u. again indicating weak Coulombic repulsion for the interaction. The NBO analysis shows that both the C–Hσ to Pd d hybrid orbital donations as well as the Pd to C–Hσ* orbital and O to C–Hσ* orbital back donation contributions can be regarded as negligible [*E*(2) values, 0.7, 1.5 and 0.2 kcal mol^{-1} respectively].

Realising that the N–Pd–N puckering for the N–C–C–N section of the ethylene diimine ring found in the energy minimised structure of **2** is somewhat unusual in terms of ethylene diamine complex bridges generally where puckering occurs at the CH_2 section[14] (see also an example later in complex **4**), we constrained the ring system to this more usual geometry to assess the effect it would have on the position of the aromatic rings with respect to the coordination plane. Figure 5 shows the resulting optimised structure **3** where it is seen that the two N atoms coordinate with one pointing slightly upwards towards the Pd coordination site and the other pointing slightly downwards.

Research Article
doi.org/10.1002/ejic.202200027

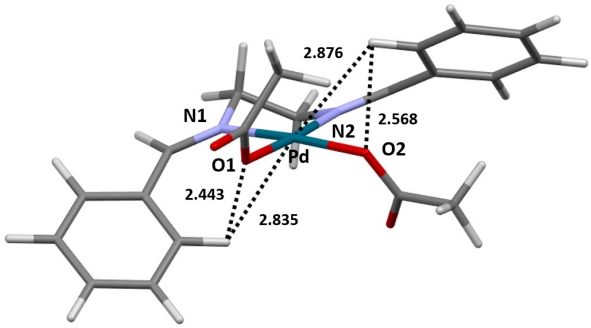

Figure 5. Calculated structure of dibenzaldimine structure **3** with CH_2 ring puckering showing the Pd···H–C and Pd···O separations (Å). Selected bond lengths (Å) and angles (°): Pd–N1 2.046, Pd–N2 2.044, Pd–O1 1.998, Pd–O2 2.018; Pd–N1=CH 134.3, Pd–N2=CH 134.5, N1=CH–C 128.9, N2=CH–C 127.9; torsion angles (°): Pd–N1=CH–C 4.3, Pd–N2=CH–C 7.8, N1=CH–C–CH 30.7, N2=CH–C–CH 32.5.

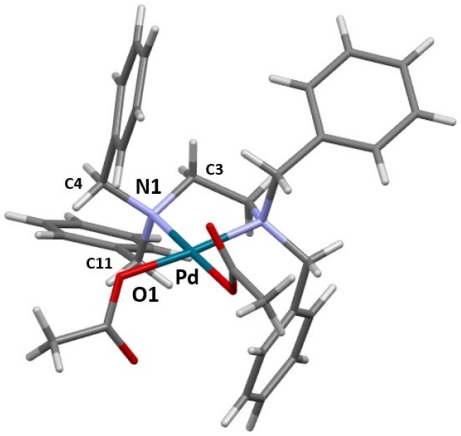

Figure 6. X-ray crystal structure of complex **4** (solvent molecules removed). Selected bond lengths (Å) and angles (°): Pd–N1 2.069(2), Pd–O1 2.025(1), N1–C3 1.492(2), N1–C4 1.512(2) N1–C11 1.519(2); Pd–N1–C3 106.8(1), Pd–N1–C4 114.4(1), Pd–N1–C11 103.7(1), N1–C3–C3′ 110.3(1), N1–C4–C5 112.2(2), N1–C11–C12 117.1(2).

This results in the relevant C=N group carbons pointing downwards at N1 and upwards at N2 so that the attached aromatic rings lie downwards below and upwards above the coordination plane in a '*transoid*' orientation. Altogether, the features observed for '*transoid*' complex **3** result in it being 27.2 kcal mol^{-1} less stable than the above-coordination plane aromatic ring complex **2**, giving in the absence of crystal structure, a good indication that the N–Pd–N puckering found in **2** would be preferred.

We have also looked at the reactions of other bidentate ligands containing the N–CH_2–CH_2–N backbone and find that the NMR spectra show a variety of reaction products, especially when the reactants are refluxed together in a solvent. In these cases, layering the NMR tube reaction with $CHCl_3$ and then a non-polar solvent, did not produce any crystalline material. However, when N,N,N′,N′-tetrabenzylethylenediamine was refluxed with $Pd(OAc)_2$ in acetic acid, the ^{1}H NMR spectrum indicated essentially a single product in which there was a downfield shifted section in the aromatic region suggesting anagostic interactions might be present in solution (Figure S2e in the ESI).

During the time the ^{13}C NMR spectra were accumulated, a yellow crystalline material precipitated from the solution, for which an X-ray structure was obtained for one crystal. Figure 6 shows the structural characteristics of this complex **4** where the coordination geometry is square planar with the *trans*-related N atoms of the chelating diamine ligand and O atoms of two terminal acetato ligands, as seen for the calculated structures **1** and **2**.

The ethylenediamine bridge system forms a 5-membered ring when the two N atoms are coordinated to Pd whereby the N–Pd–N–CH_2 section of the ring is essentially planar. The puckering occurs by way of the remaining CH_2 group which differs from the calculated structure **2** where the puckering involved the N–Pd–N section of the ring and the N–CH_2–CH_2–N ring section was essentially planar and is similar to that found in structure **3**. With the ring puckered in this way, one benzyl group attached to N1 lies above the coordination plane with the other lying backwards underneath the coordination plane and locally underneath the N1–CH_2 carbon which forms the upwards section of the ring puckering. This process is repeated at the other N atom except that one benzyl group lies below the coordination plane with the other one lying backwards over the coordination plane and locally over the N2–CH_2 carbon. A similar positioning of the benzyl groups has been found for this ligand coordinated to $CuCl_2$.[15]

With the C_2 symmetry present in the molecule the upper and lower sections of the structure containing the aromatic rings are identical. The *'transoid'* orientation of the two frontal benzylic groups is similar to that found in N_2PdCl_2 complexes containing an ethylene diamine bridge and a single benzylic group on each N atom.[16] For the upper and lower frontal benzylic groups in **4**, the aromatic rings are rotated so that one *ortho*-hydrogen of each aromatic ring sits over or underneath the O1 or the other O atom of the acetato ligands (Figure 7) and with the symmetry relationship within the molecule, the metrics are the same for both. Thus, considering the N1 frontal benzylic group, the O1···H–C separation is 2.346 Å but with the H- atom sitting more over O1 than Pd, the Pd···H–C separation is long at 2.869 Å. In addition, the symmetry-related acetato ligand is rotated so that the C=O group oxygen points obliquely towards the *ortho*-C–H hydrogen but the separation is long at 2.933 Å. In solution, these rings would be rapidly rotating on the NMR time scale, so that the *ortho*-hydrogens would come closer to the Pd centre than the X-ray structure shows. However, the *ortho*-hydrogens in the ^{1}H NMR spectrum are not shifted downfield to the extent found for the diimine ligand complexes so that well developed anagostic interactions may not occur. No computational analysis was undertaken for complex **4** due to the large Pd···H–C separation found in the X-ray structure.

Research Article
doi.org/10.1002/ejic.202200027

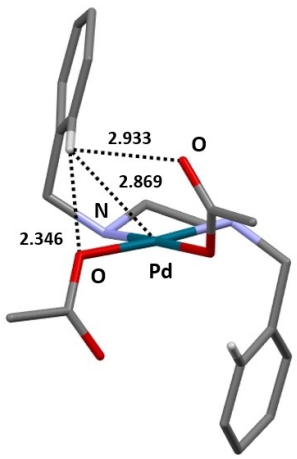

Figure 7. Pd···H–C and O···H–C separations (Å) in the X-ray crystal structure of complex **4** using the aromatic ring C–H bond length at the X-ray structure calculated length of 0.093 Å.

Conclusions

The results of this work show that when a variety of aromatic ring N,N′-chelate ligands are reacted with $Pd(OAc)_2$ under forcing conditions such as long reflux periods in MeOH or HOAc, NMR spectra show a range of products form without a single end-product result. When the back-bone section of an aromatic diimine N,N′ chelate has 3 carbons, stirring the diimine ligand with $Pd(OAc)_2$ in MeOH or $CHCl_3$ which are conditions that would normally bring about cyclopalladation for ligands containing a single coordinating atom such as in Me_2NCH_2Ph, the NMR spectra of the solids obtained show that the reactions do not appear to progress towards cyclometallation but appear to halt at an anagostic stage. When the aromatic diimine back bone is changed to the two-carbon CH_2–CH_2 system, the reaction seems to progress further past the *bis*-anagostic stage but no single end product is again forthcoming. Although no publishable X-ray data was obtained for this type of structure, DFT calculations pointed to an above plane *bis*-anagostic situation. In another reaction using the CH_2–CH_2 backbone but where benzyl groups were present, a weak *bis*-anagostic structure was indicated in solution by the ^{1}H NMR spectrum and the X-ray structure showed above and below plane *ortho*-hydrogens sitting more over the acetato ligand coordinated oxygen atoms than the palladium centre.

The NMR spectra of the progressing reactions show that although there is coordination of the chelating ligand, the reaction does not appear to progress much after the initial coordination event when the *bis*-anagostic complex is formed. To proceed further, an *ortho*-hydrogen would need to move into the coordination plane to form an agostic interaction and delocalise the C–H bond electron density. To achieve this event, an acetato ligand would need to dissociate to form a cationic intermediate or, in a concerted process such as that involving a CMD/AMLA mechanism,[10] the acetato ligand would need to assist the removal of the hydrogen at the same time as the Pd–C bond formed. However, neither of these processes appear to occur to any extent based on the apparent reluctance of the system to produce a Pd–C bond and certainly not C–Pd–C bonds. It is noted that in the *bis*-anagostic structures found for the present complexes, the C=O oxygen atoms of the acetato ligands do not participate in close approaches to any of the *ortho*-aromatic ring hydrogens that might then lead on to removal of the ligand as HOAc. Further work is at present underway to attempt to resolve this problem.

Experimental Section

Experimental Details

Materials and methods. Palladium acetate, 2,2-dimethyl-1,3-diaminopropane, ethylene diamine, benzaldehyde, *para-tert*-butylbenzaldehyde and benzyl chloride were obtained from Aldrich and used as received. Commercial grade solvents were used without purification. The diimine ligands were prepared by refluxing 1 equivalent of 2,2-dimethyl-1,3-diaminopropane or ethylene diamine with two equivalents of benzaldehyde or *para-tert*-butylbenzaldehyde in ethanol and the mixtures refluxed overnight. Removing the solvent until either liquid or solid products were obtained gave the ligands in sufficient purity for further use. N,N,N′,N′-tetrakis(phenylmethyl)-1,2-ethanediamine was prepared by refluxing 7 mL of ethylenediamine with 8 g of NaOH and 30 mL of benzyl chloride in 20 mL of water for 4 hours and collecting the white solid that formed on cooling.[15,17] Reactions between $Pd(OAc)_2$ and the ligand were carried out in a 1:1 ratio on a 0.223 mmole scale [0.05 g $Pd(OAc)_2$] in the appropriate solvent which was stripped off at the end of the reaction after filtering. NMR spectra were then run in $CDCl_3$ and on completion, the NMR tube was layered with an equivalent amount of $CHCl_3$ and then diethyl ether or another suitable non-polar solvent. The NMR tube was then capped and allowed to stand to produce crystals. NMR spectra were obtained on a Bruker Avance 300 s spectrometer.

Crystallographic data. To prevent loss of solvent from the crystalline products, the crystalline material was removed directly from the NMR tube and mounted immediately on the diffractometer. The X-ray data were collected on a Siemens Bruker instrument with graphite-monochromated Mo–Kα radiation (λ = 0.71073 Å) at T = 150(2) K. The structure was solved and refined on all F^2 with programs SHELXT[18] and SHELXL[19] in the OLEX2 package.[20]

Crystal data for complex 3: $C_{17}H_{19}NO_2Pd_{0.5}.2(CHCl_3)$; monoclinic, space group C2/c, $a = 25.9312(4)$, $b = 10.83453(14)$, $c = 17.8416(3)$, $\beta = 108.7249(17)$ Å, $V = 4747.3$ (1) Å^3, Z = 8,, $D_c = 1.571$ g cm^{-1}, μ (Cu–Kα) = 9.70 mm^{-1}, crystal size = 0.10 × 0.10 × 0.05 mm, θ max = 67.684°, *R*(int) 0.0457, *F(000)* = 2264, 4771 unique reflections, 259 parameters refined, $R_1 = 0.0269$, $F_o > 4\sigma(F_o)$ for 4313 reflections, *wR2* = 0.0646. Crystallographic data have been deposited with the Cambridge Crystallographic Data Center, CCDC number 2114528.

Computational details. Density functional theory (DFT) based geometry optimizations and vibrational calculations for the complexes were performed using the dispersion corrected PBE–D3[21,22] functional within the Gaussian16 (G16)[23] software. A triple-zeta high quality basis set (aug-cc-pVTZ-PP)[24] was employed for Pd together with a scalar relativistic energy consistent Stuttgart pseudopotentials for Pd; cc-pVTZ[25] for the attached ancillary ligands (O atoms), anagostic hydrogen and nitrogen (attached to the metals) and double-zeta quality basis set (cc-pVDZ)[25] was used for the remainder of atoms. No imaginary frequencies were found in the vibrational analysis. All complexes were treated as singlet

states. The NBO calculations were performed with the NBO7.0 package.[26] For the QTAIM analyses, the input files (.wfx) were obtained from G16[23] and the QTAIM calculations were performed with the AIMALL software.[27] For structure **1** the initial complex was drawn in the Gaussian program with both aromatic rings above the coordination plane and no preferred conformation of the coordinated propylene diimine ring based on molecular models that indicated an above and below plane disposition of the aromatic rings would lead to an improbable boat ring structure. For structure **2** the initial complex was drawn with no preferred N–CH_2–CH_2–N ring conformation and with the aromatic rings in an above-plane position. For structure **3** the structure was drawn as for complex **2** but with the aromatic rings in above and below plane positions. For complex **4**, no preferred conformation of the N–CH_2–CH_2–N ring or positioning of the aromatic rings was used.

Deposition Number 2114528 (for **4**) contains the supplementary crystallographic data for this paper. These data are provided free of charge by the joint Cambridge Crystallographic Data Centre and Fachinformationszentrum Karlsruhe Access Structures service www.ccdc.cam.ac.uk/structures.

Supporting Information (see the footnote on the first page of this article): Mercury diagrams for **1**–**4**, ^{1}H NMR spectra, torsion angles for **1**, QTAIM molecular graphs, metrics, QTAIM atomic charge and NBO data for **1** and **2**. The mercury diagrams are available as separate files under Supporting Information.

Acknowledgements

Open access publishing facilitated by Massey University, as part of the Wiley - Massey University agreement via the Council of Australian University Librarians.

Conflict of Interest

The authors declare no conflict of interest.

Data Availability Statement

The data that support the findings of this study are available in the supplementary material of this article.

Keywords: *bis*-Anagostic interactions · C–H bond activation · Cyclometallation reactions · Palladium

[1] See for example: a) M. Pfeffer, *Pure Appl. Chem.* **1992**, *64*, 335–342; b) I. Omae, *Coord. Chem. Rev.* **2004**, *248*, 995–1023; c) A. D. Ryabov, *Synthesis* **1985**, 233–252; d) J. Dupont, M. Pfeffer, J. Spencer, *Eur. J. Inorg. Chem.* **2001**, 1917–1927; e) R. B. Bedford, *Chem. Commun.* **2003**, 1787–1796; f) J. Dupont, C. S. Consorti, J. Spencer, *Chem. Rev.* **2005**, *105*, 2527–2571; g) J. P. Djukic, J. B. Sortais, L. Barloy, M. Pfeffer, *Eur. J. Inorg. Chem.* **2009**, 817–853; h) M. Albrecht, *Chem. Rev.* **2010**, *110*, 576–623; i) L. Cuesta, E. P. Urriolabeitia, *Comments Inorg. Chem.* **2012**, *33*, 55–85.

[2] a) T. W. Lyons, M. S. Sanford, *Chem. Rev.* **2010**, *110*, 1147–1169; b) O. Baudoin, *Chem. Soc. Rev.* **2011**, *40*, 4902–4911; c) K. M. Engle, T.-S. Mei, M. Wasa, J.-U. Qu, *Acc. Chem. Res.* **2012**, *45*, 788–802; d) A. F. M. Noisier, M. A. Brimble, *Chem. Rev.* **2014**, *114*, 8775–8806; e) G. Rouquet, N. Chatani, *Angew. Chem. Int. Ed.* **2013**, *52*, 11726–11743 and refs cited therein; f) I. P. Beletskaya, A. V. Cheprakov, *J. Organomet. Chem.* **2004**, *689*, 4055–4082.

[3] For Ni C–H bond activation and cyclometallation reactions, see the references in the introduction of reference 13. For reviews relevant to Ni promoted C–H bond activation see: a) S. Z. Tasker, E. A. Standley, T. F. Jamison, *Nature* **2014**, *509*, 299–309; b) M. Tobisu, N. Chatani, *Acc. Chem. Res.* **2015**, *48*, 1717–1726; c) M. Marín, R. J. Rama, M. C. Nicasio, *Chem. Rec.* **2016**, *16*, 1819–1832; d) L. Yu, C. Yang, Y. Yu, D. Liu, L. Hu, Y. Xiao, Z.-N. Song, Z. Tan, *Org. Lett.* **2019**, *21*, 5634–5638; For Co see e) Y. Commagalla, N. Chatani, **2017**, *350*, 117–135; f) M. Moselage, J. Li, L. Ackermann, *ACS Catal.* **2016**, *6*, 498–525; g) D. Wei, X. Zhu, J.-L. Niu, M.-P. Song, *ChemCatChem.* **2016**, *8*, 1242–1263; h) N. Yoshikai, *J. Synth. Org. Chem. Jpn.* **2014**, *72*, 1198–1206; i) T. Yoshino, S. Matsunaga, *Adv. Synth. Catal.* **2017**, *359*, 1245–1262.

[4] a) D. C. Powers, D. Y. Xiao, M. A. L. Geibel, T. Ritter, *J. Am. Chem. Soc.* **2010**, *132*, 14530–14536; b) P. Jolliet, M. Gianini, A. von Zelewsky, G. Bernardinelli, H. Stoeckli-Evans, *Inorg. Chem.* **1996**, *35*, 4833–4888; c) A. Kasahara, T. Izumi, *Bull. Chem. Soc. Jpn.* **1969**, *42*, 1765–1766; d) G. Longoni, P. Fantucci, P. Chini, F. Camziani, *J. Organomet. Chem.* **1972**, *39*, 413–425; e) S. Trofimenko, *Inorg. Chem.* **1973**, *12*, 1215–1221; f) C. Arlen, M. Pfeifer, O. Bars, D. Grandjean, *J. Chem. Soc. Dalton Trans.* **1983**, 1535–1544; g) A. C. Cope, R. N. Gourley, *J. Organomet. Chem.* **1967**, *8*, 527–533; h) T. Janecki, J. A. D. Jeffreys, P. L. Pauson, A. Pietrzykowski, *Organometallics* **1987**, *6*, 1553–1560.

[5] A. F. M. J. van der Ploeg, G. van Koten, K. Vrieze, *J. Organomet. Chem.* **1981**, *222*, 155–174.

[6] a) G. R. Newkome, V. K. Gupta, F. R. Fronczek, *Organometallics* **1982**, *1*, 907–910; b) G. R. Newkome, W. E. Puckett, V. K. Gupta, F. R. Fronczek, *Organometallics* **1983**, *2*, 1247–1249.

[7] a) M. M. Bagga, W. T. Flannigan, G. R. Knox, P. L. Pauson, *J. Chem. Soc. C* **1969**, 1534–1537; b) C. Werlé, L. Karmazin, C. Bailly, L. Ricard, J.-P. Djukic, *Organometallics* **2015**, *34*, 3055–3064.

[8] M. G. Clerici, B. L. Shaw, B. Weeks, *J. C. S. Chem. Comm.* **1973**, 516–517.

[9] a) Q. Zhao, G. Meng, S. P. Nolan, M. Zsostak, *Chem. Rev.* **2020**, *120*, 1981–2048; b) J. Diesel, N. Cramer, *ACS Catal.* **2019**, *9*, 9164–9177; c) G. Xia, J. Weng, L. Liu, P. Verma, Z. Li, J.-Q. Yu, *Nat. Chem.* **2019**, *11*, 571–577.

[10] a) D. L. Davies, S. M. A. Donald, S. A. Macgregor, *J. Am. Chem. Soc.* **2005**, *127*, 13754–13755; b) D. L. Davies, S. A. Macgregor, C. L. McMullin, *Chem. Rev.* **2017**, *117*, 8649–8709; c) B. P. Carrow, J. Sampson, L. Wang, *Isr. J. Chem.* **2019**, *59*, 1–30.

[11] a) M. A. Sajjad, K. E. Christensen, N. H. Rees, P. Schwerdtfeger, J. A. Harrison, A. J. Nielson, *Dalton Trans.* **2017**, *46*, 16126–16138; b) A. J. Nielson, *J. Chem. Soc. Dalton Trans.* **1981**, 205–211; c) J. A. Harrison, A. J. Nielson, M. A. Sajjad, G. C. Saunders, P. Schwerdtfeger, *Eur. J. Inorg. Chem.* **2016**, 64–77; d) A. J. Nielson, J. A. Harrison, M. A. Sajjad, P. Schwerdtfeger, *Eur. J. Inorg. Chem.* **2017**, 2255–2264; e) M. A. Sajjad, P. Schwerdtfeger, J. A. Harrison, A. J. Nielson, *Eur. J. Inorg. Chem.* **2017**, 5485–5496; f) K. Ha, *Z. Kristallogr.* **2011**, *226*, 501–502; g) J. Vázquez, S. Bernès, P. Sharma, J. Pérez, G. Hernández, A. Tovar, U. Peña, R. Gutiérrez, *Polyhedron* **2011**, *30*, 2514–2522; h) K. A. Pelz, P. S. White, M. R. Gagne, *Organometallics* **2004**, *23*, 3210–3217.

[12] a) R. F. W. Bader in *Atoms in Molecules: A Quantum Theory*, The Clarendon Press, Oxford, **1990**; b) R. F. W. Bader, *Chem. Rev.* **1991**, *91*, 893–928; c) P. Popelier in *Atoms in Molecules: An Introduction*, Prentice Hall, Pearson Education Ltd, **2000**; d) M. Jablonski, *ChemistryOpen* **2019**, *18*, 497–507.

[13] a) F. Weinhold, C. Landis, *Valency and bonding: A Natural Bond Orbital Donor-Acceptor Perspective;* Cambridge University Press, Cambridge, England, **2005**; b) F. Weinhold, C. Landis, E. D. Glendenning, *Int. Rev. Phys. Chem.* **2016**, *35*, 399–440.

[14] a) T. H. Noh, S. M. Kim, K. H. Park, O.-S. Jung, *Transition Met. Chem.* **2012**, *37*, 535–540; b) A. C. Moro, F. W. Watanabe, S. R. Ananias, A. E. Mauro, A. V. G. Netto, A. P. R. Lima, J. G. Ferreira, R. H. A. Santos, *Inorg. Chem. Commun.* **2006**, *9*, 493–496; c) P. L. Alsters, P. F. Engel, M. P. Hogerheide, M. Copijn, A. L. Spek, G. van Koten, *Organometallics* **1993**, *12*, 1831–1844.

[15] a) J. Kaizer, Z. Zsigmond, I. Ganszky, G. Speier, M. Giorgi, M. Reglier, *Inorg. Chem.* **2007**, *46*, 4660–4666; b) H. Guan, Z. Wang, A. Famulari, X. Wang, F. Guo, J. Martí-Rujas, *Inorg. Chem.* **2014**, *53*, 7438–7445.

[16] K. A. Pelz, P. S. White, M. R. Gagne, *Organometallics* **2004**, *23*, 3210–3217.

[17] F. Guo, Z. Wang, J.-J. Zhang, A. Famulari, H. Lia, J. Martí-Rujas, *Dalton Trans.* **2017**, *46*, 9466–9471.

[18] G. M. Sheldrick, *Acta Crystallogr.* **2015**, *A71*, 3–8.

Research Article
doi.org/10.1002/ejic.202200027

[19] G. M. Sheldrick, *Acta Crystallogr.* **2015**, *C71*, 3–8.
[20] O. V. Dolomanov, L. J. Bourhis, R. J. Gildea, J. A. K. Howard, H. Puschmann, *J. Appl. Crystallogr.* **2009**, *42*, 339–341.
[21] J. P. Perdew, K. Burke, M. Ernzerhof, *Phys. Rev. Lett.* **1996**, *77*, 3865–3868.
[22] S. Grimme, J. Antony, S. Ehrlich, H. Krieg, *J. Chem. Phys.* **2010**, *132*, 154104–154119.
[23] Gaussian 16, Revision A.03, M. J. Frisch, G. W. Trucks, H. B. Schlegel, G. E. Scuseria, M. A. Robb, J. R. Cheeseman, G. Scalmani, V. Barone, G. A. Petersson, H. Nakatsuji, X. Li, M. Caricato, A. V. Marenich, J. Bloino, B. G. Janesko, R. Gomperts, B. Mennucci, H. P. Hratchian, J. V. Ortiz, A. F. Izmaylov, J. L. Sonnenberg, D. Williams-Young, F. Ding, F. Lipparini, F. Egidi, J. Goings, B. Peng, A. Petrone, T. Henderson, D. Ranasinghe, V. G. Zakrzewski, J. Gao, N. Rega, G. Zheng, W. Liang, M. Hada, M. Ehara, K. Toyota, R. Fukuda, J. Hasegawa, M. Ishida, T. Nakajima, Y. Honda, O. Kitao, H. Nakai, T. Vreven, K. Throssell, J. A. Montgomery, Jr., J. E. Peralta, F. Ogliaro, M. J. Bearpark, J. J. Heyd, E. N. Brothers, K. N. Kudin, V. N. Staroverov, T. A. Keith, R. Kobayashi, J. Normand, K. Raghavachari, A. P. Rendell, J. C. Burant, S. S. Iyengar, J. Tomasi, M. Cossi, J. M. Millam, M. Klene, C. Adamo, R. Cammi, J. W. Ochterski, R. L. Martin, K. Morokuma, O. Farkas, J. B. Foresman, D. J. Fox, Gaussian, Inc., Wallingford CT, **2016**.
[24] K. A. Peterson, D. Figgen, M. Dolg, H. Stoll, *J. Chem. Phys.* **2007**, *126*, 124101–124112.
[25] T. H. Jr. Dunning, *J. Chem. Phys.* **1989**, *90*, 1007–1023.
[26] NBO 7.0. E. D. Glendening, J, K. Badenhoop, A. E. Reed, J. E. Carpenter, J. A. Bohmann, C. M. Morales, P. Karafiloglou, C. R. Landis, F. Weinhold, Theoretical Chemistry Institute, University of Wisconsin, Madison, **2018**.
[27] AIMAll (version 16.08.17), T. A. Keith, TK Gristmill Software, Overland Park KS, USA, **2016**, http://aim.tkgristmill.com.

Manuscript received: January 17, 2022
Revised manuscript received: February 21, 2022
Accepted manuscript online: February 27, 2022